Cell Reports
Resource

Human Stem Cell-Derived Spinal Cord Astrocytes with Defined Mature or Reactive Phenotypes

Laurent Roybon,[1,2,7] Nuno J. Lamas,[1,2,6,8] Alejandro Garcia-Diaz,[1,6] Eun Ju Yang,[5] Rita Sattler,[5] Vernice Jackson-Lewis,[2] Yoon A. Kim,[1] C. Alan Kachel,[1] Jeffrey D. Rothstein,[5] Serge Przedborski,[2] Hynek Wichterle,[1,2,3] and Christopher E. Henderson[1,2,3,4,*]

[1]Project A.L.S./Jenifer Estess Laboratory for Stem Cell Research, Columbia University Medical Center, P&S 16-440, 630 West 168th Street, New York, NY 10032, USA
[2]Columbia Stem Cell Initiative (CSCI), Departments of Pathology and Cell Biology and Neurology, Center for Motor Neuron Biology and Disease (MNC), Columbia University Medical Center, P&S 5-420, 630 West 168th Street, New York, NY 10032, USA
[3]Department of Neuroscience, Columbia University Medical Center, P&S 5-420, 630 West 168th Street, New York, NY 10032, USA
[4]Department of Rehabilitation and Regenerative Medicine, Columbia University Medical Center, P&S 5-420, 630 West 168th Street, New York, NY 10032, USA
[5]Brain Science Institute and Department of Neurology, Johns Hopkins University, 855 N Wolfe Street, Rangos 2-223, Baltimore, MD 21205, USA
[6]These authors contributed equally to this work
[7]Present address: Stem Cell Laboratory for CNS Disease Modeling, Department of Experimental Medical Science, Lund University, Lund 22184, Sweden
[8]Present address: Life and Health Sciences Research Institute (ICVS), School of Health Sciences, University of Minho Braga, Portugal
*Correspondence: ch2331@columbia.edu
http://dx.doi.org/10.1016/j.celrep.2013.06.021

SUMMARY

Differentiation of astrocytes from human stem cells has significant potential for analysis of their role in normal brain function and disease, but existing protocols generate only immature astrocytes. Using early neuralization, we generated spinal cord astrocytes from mouse or human embryonic or induced pluripotent stem cells with high efficiency. Remarkably, short exposure to fibroblast growth factor 1 (FGF1) or FGF2 was sufficient to direct these astrocytes selectively toward a mature quiescent phenotype, as judged by both marker expression and functional analysis. In contrast, tumor necrosis factor alpha and interleukin-1β, but not FGFs, induced multiple elements of a reactive inflammatory phenotype but did not affect maturation. These phenotypically defined, scalable populations of spinal cord astrocytes will be important both for studying normal astrocyte function and for modeling human pathological processes in vitro.

INTRODUCTION

Astrocytes play multiple roles in the central nervous system (CNS). Many of these are critical to normal function in the healthy adult, where astrocytes act as support cells for neurons, regulating cerebral blood flow, energy reserves, and neurogenesis (Abbott, 1988; Allaman et al., 2011; Lie et al., 2005; Okamoto et al., 2011; Takano et al., 2006). Moreover, their involvement in synaptic transmission and plasticity has been the object of intensive study (Bernardinelli et al., 2011; Panatier et al., 2011). Cell culture models used to study normal astrocyte function should therefore reflect this mature, quiescent phenotype.

However, astrocyte phenotypes are extremely dynamic. Reactive phenotypes can be induced by proinflammatory factors, such as tumor necrosis factor alpha (TNFα), interleukin (IL)-1β, and interferon gamma, in a wide variety of traumatic and pathological contexts (Gwak et al., 2012). Indeed, multiple classes of reactive astrocytes can be identified, depending on the nature of activating stimulus and the time elapsed postactivation (Zamanian et al., 2012). Astrocyte activation leads to production of a wide array of mediators, including chemokines, inflammatory cytokines, and growth factors (Allaman et al., 2011), as well as transcriptional changes of genes associated with cell-to-cell communication (e.g., connexins), cytoskeletal structure (e.g., glial fibrillary acidic protein [GFAP]), and many others (for review, see Sofroniew [2009]). It is therefore essential to precisely model the reactive state for in vitro studies of human disease.

Human astrocytes have been cultured from fetal or adult postmortem CNS using expansion of neural precursors (Caldwell et al., 2001; Haidet-Phillips et al., 2011; Lee et al., 1993; Verwer et al., 2007), but such preparations are rare and intrinsically variable. One of the first protocols to report differentiation of human embryonic stem cells (hESCs) into astrocytes was that of Krencik et al. (2011). However, one practical drawback of the method is that it necessitates 6 months of culture to generate a sufficiently pure population (Krencik et al., 2011; Krencik and Zhang, 2011). Since then, other protocols starting from neural precursor cells have reported generation of astrocytes within 35–80 days (Emdad et al., 2012; Juopperi et al., 2012; Lafaille et al.,

2012; Serio et al., 2013; Shaltouki et al., 2013). However, by the criteria discussed below, the astrocytes generated in each case are immature and do not fully model normal astrocyte function.

Astrocyte maturation occurs through a complex series of events that remain incompletely understood. There is considerable overlap between expression of different markers, and it is likely that the precise sequence of their appearance varies from one region of the CNS to another. Nevertheless, we have constructed a tentative synthesis of the appearance of known markers during maturation based on spinal cord data, where available (Figure S1). Overall, astrocyte development and maturation encompasses two phases (see Extended Results for full review, abbreviations, and citations). During the first—mainly embryonic—phase, subsets of astrocytes are generated from radial glia and progressively take on their principal functional phenotypes. Subsequently, over the first postnatal weeks in rodents, astrocytes adopt a mature, quiescent morphology and phenotype. Although all potential marker genes have not been studied in parallel in a single brain region, the sequence of appearance of markers during the first, embryonic phase is likely NF1A > GLAST > ALDH1L1 > Cx43 > S100β > CD44 > AldolaseC > GFAP. The $NF1A^+/GFAP^+$ cells generated by extant stem cell differentiation protocols (see above) likely correspond to this first, immature stage. In contrast, the second, maturational phase is associated with downregulation of GFAP, GLAST, and ALDH1L1, whereas GFAP expression persists in white matter astrocytes. In parallel, there is continued accumulation of Cx43, followed by Aqp4 and the mature astrocyte glutamate transporter 1 (GLT1). Therefore, mature gray matter astrocytes should not be expected to express high levels of GFAP, so other markers are needed to monitor their maturation and purity.

To summarize, astrocytes may adopt either a quiescent state with protoplasmic morphology, characterized by low GFAP and high GLT1, or a fibrous, reactive phenotype characterized by high GFAP and low GLT1. Standard preparations of cultured $GFAP^+$ astrocytes (McCarthy and de Vellis, 1980) reflect only the latter (Zamanian et al., 2012). Therefore, a robust model of mature, quiescent astrocytes would be a significant step forward for in vitro studies of human neural function as well as disease. This is especially significant given the different effects of immature and mature astrocytes on axonal regeneration (Goldshmit et al., 2012; Tom et al., 2004). Here, we report that, using identified signaling factors, mouse or human spinal cord astrocytes generated from either ESCs or human induced pluripotent stem cells (hiPSCs) can be induced to adopt phenotypes that correspond to those of either mature or reactive astrocytes in vivo. Such defined populations of mature human astrocytes will considerably increase the resolution of studies of normal astrocyte function, whereas fully activated preparations open the door to more precise disease modeling based on patient-derived hiPSCs.

RESULTS

Astrocytes Derived from Mouse Embryonic Stem Cells Are Immature

Because the development and maturation of astrocytes are better understood in rodents than in human, we first generated astrocytes from mouse embryonic stem cells (mESCs). Our overall aim was to generate astrocytes of spinal cord identity as a tool for modeling motor neuron diseases, such as amyotrophic lateral sclerosis (ALS). We therefore used an induction protocol that specifies ventral spinal progenitors (Wichterle et al., 2002) followed by neurosphere expansion, which amplifies neural progenitors and generates largely glial cells (Kuegler et al., 2012; Figure S1; Experimental Procedures). After 1 week, cultures of dissociated neurospheres contained cells that stained for canonical markers of developing astrocytes: GFAP, Aqp4, S100β, vimentin, and NF1A (Figures 1A and 1B), and their spinal cord identity was confirmed by coexpression of HoxB4 (Figure 1A). The pluripotency marker Oct4 was undetectable (Figure S2C), and neurons (βIII-tubulin$^+$), microglia (Iba1$^+$), and oligodendrocytes (2′3′-cyclic-nucleotide 3′-phosphodiesterase [CNPase]$^+$ or oligodendrocyte transcription factor 2 [Olig2]$^+$) were rare or absent (Figures 1B and S1D). The mESC-derived cultures therefore contained essentially only astrocytes and glial precursors. However, they were not homogeneous, because many cells were not double stained for any given pair of antigens (Figure 1A) and less than one-third of the cells positive for vimentin and NF1A expressed the markers Aqp4, S100β, or GFAP (Figure 1B). This is comparable to the heterogeneity in cultures of neonatal astrocytes (Imura et al., 2006). Our data suggested that the cultures contained developing astrocytes at different stages of maturity.

To assess their state of maturation, we used western blots to quantify levels of three markers known to be upregulated in astrocytes as they mature: GLAST and ALDH1L1, which appear at midembryogenesis, and GLT1, a postnatal marker (Figure 1C; see Extended Results). Although 4 weeks had elapsed since the mESCs were put into culture, and although GFAP was clearly present, none of these markers could be detected. This was in contrast to astrocytes generated from primary neural precursors of embryonic day 12.5 (E12.5) spinal cords using a neurosphere-based approach (Figure S2A), which expressed robust levels of GLAST, ALDH1L1, and GLT1 (Figure 1C). We therefore sought treatments through which mESC-derived spinal astrocytes could be brought to a similar degree of maturity.

FGFs Promote Maturation of mESC-Derived Astrocytes

In vivo, fibroblast growth factors (FGFs) have been proposed to act as differentiation signals for astrocytes (Irmady et al., 2011; Morrow et al., 2001) and FGF1 is strongly expressed in postnatal spinal neurons (Elde et al., 1991). Addition of FGF1 to mESC-derived astrocytes from days 28–35 triggered a >4-fold increase in the number of cells expressing GLT1, with an EC_{50} of 5 ng/ml (Figures 2A and 2B). Similar results were obtained using FGF2 in place of FGF1 (Figure S3). Western blotting confirmed that FGF increased overall levels of both GLT1 and GLAST (Figures 2C, 2D, and S3C) as well as other maturation markers, such as aldolase C, Cx43, and ALDH1L1 (Figures 2D and S3C). In parallel, GFAP levels were strongly downregulated (Figures 2B, 2D, S3A, and S3C). Thus, mESC-derived cultures treated with FGFs express high levels of glutamate transporters and low GFAP, a phenotype reminiscent of mature quiescent astrocytes.

To determine whether this biochemical maturation resulted in functional changes, we measured glutamate uptake, a key role

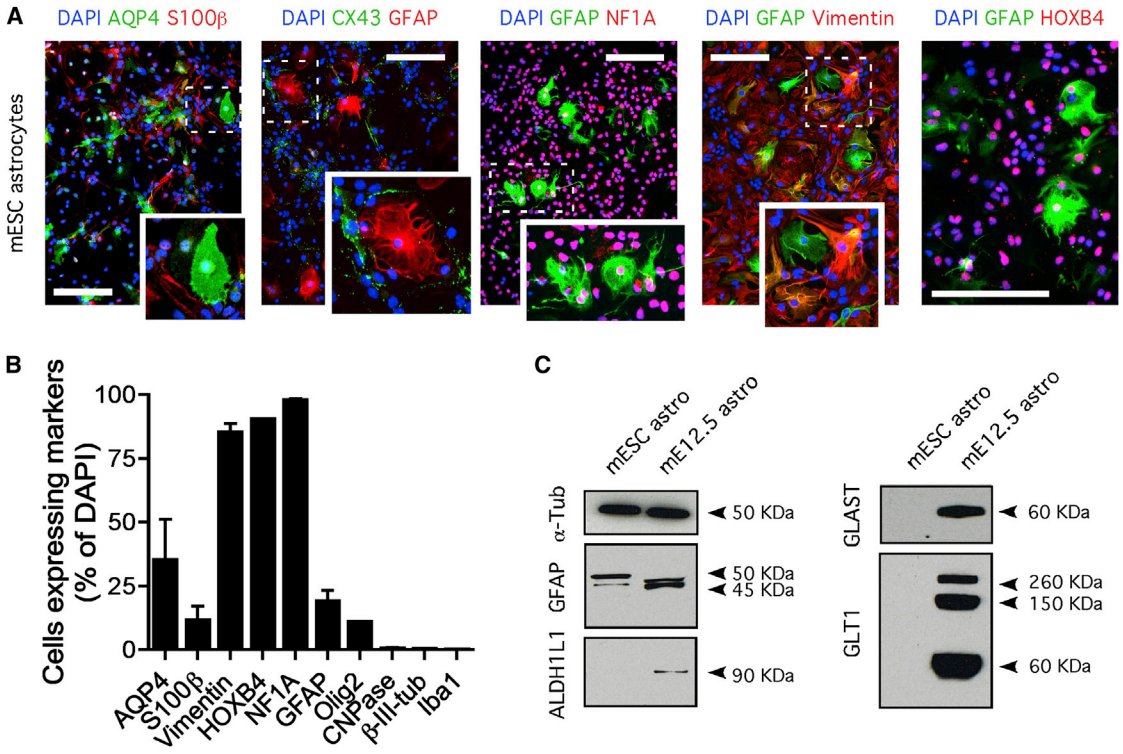

Figure 1. Mouse ESC-Derived Spinal Cord Astrocytes Show an Immature Phenotype

(A) Differentiated mESC cultures contain glial cells expressing canonical astrocyte markers together with the spinal cord marker HOXB4. Insets show higher magnification of regions indicated with dotted lines. The scale bars represent 75 μm.

(B) Percentages of mESC-derived glial cells expressing markers for astroglia (Aqp4, S100β, vimentin, NF1A, and GFAP), oligodendroglia (Olig2 and CNPase), neurons (β-III-tubulin), microglia (Iba1), and spinal cord identity (HOXB4). Mean ± SEM; n = 3–4 independent differentiations.

(C) Western blot of mESC-derived astrocytes as compared to astrocytes derived from E12.5 mouse embryo spinal cord. GFAP protein is present in both, but ALDH1L1, GLAST, and GLT1 are only detectable in the mE12.5-derived astrocytes. α-tubulin was used as loading control.

See also Figure S2.

of mature astrocytes (Huang and Bergles, 2004). In mESC astrocytes from two different cell lines grown in fetal bovine serum (FBS) alone, we detected significant levels of glutamate uptake that were Na^+-dependent, as expected (Figure 2E; Mitani and Tanaka, 2003; Rothstein et al., 1996). Exposure to FGF1 for 7 days led to a 2-fold increase in glutamate transport (Figure 2E), reflecting upregulation of the transporters responsible (Figures 2B–2D). Thus, functional astrocytes can be efficiently generated from mESCs and FGF1 promotes their biochemical and functional maturation to a quiescent state.

Human Spinal Cord Astrocytes Derived from hESCs and hiPSCs following Early Neuralization

We then used the findings with mouse ESCs to generate mature human astrocytes. To accelerate astrocyte production, rather than passing through a stage of cycling neural precursors (Shaltouki et al., 2013), we turned to early neuralization by dual inhibition of SMAD signaling, which had been shown by Chambers et al. (2009) to enhance production of CNS precursors and neurons but whose effect on glial generation had not been studied. To inhibit SMAD signaling, we employed the activin receptor-like kinase 4 (ALK4)/ALK5/ALK7 inhibitor SB431542 together with LDN193189, a potent derivative of dorsomorphin that inhibits transforming growth factor β1/activin receptor-like kinase (Boulting et al., 2011; Kriks et al., 2011; Yu et al., 2008).

We used one hESC line (R1; James et al., 2006) and one hiPSC line (18c; Bock et al., 2011; Boulting et al., 2011) derived from a healthy volunteer, which we have shown to have a strong propensity for neural differentiation. When SB431542 (10 μM) and LDN193189 (0.2 μM) were added to cultures from 1 to 5 days in vitro (DIV) (Figure 3A), 70%–80% of cells in the culture at 10 DIV were $PAX6^+$ $Oct4^-$ neural progenitors (data not shown). To direct the cells toward a caudal ventral identity, retinoic acid (RA) and sonic hedgehog cysteine mutated (SHH-C) were added, as indicated, and neurotrophic factors were provided to support neuronal survival (Figure 3A). By 40 DIV, as with earlier protocols (Hu et al., 2010; Karumbayaram et al., 2009; Li et al., 2005; Shaltouki et al., 2013), the cultures were enriched for markers of ventral neuronal populations (OLIG2, HB9, ISL1/ISL2, NKX2.2, and NKX6.1; data not shown). Critically for our studies, they showed spinal cord (HOXB4; >90%) but not midbrain (OTX2; <2%) identity (Figure 3B). Early neuralization did not, therefore, perturb the patterning of these neural precursors.

We monitored the appearance of different cell classes over the course of culture in FBS (1%) of these and two further hESC

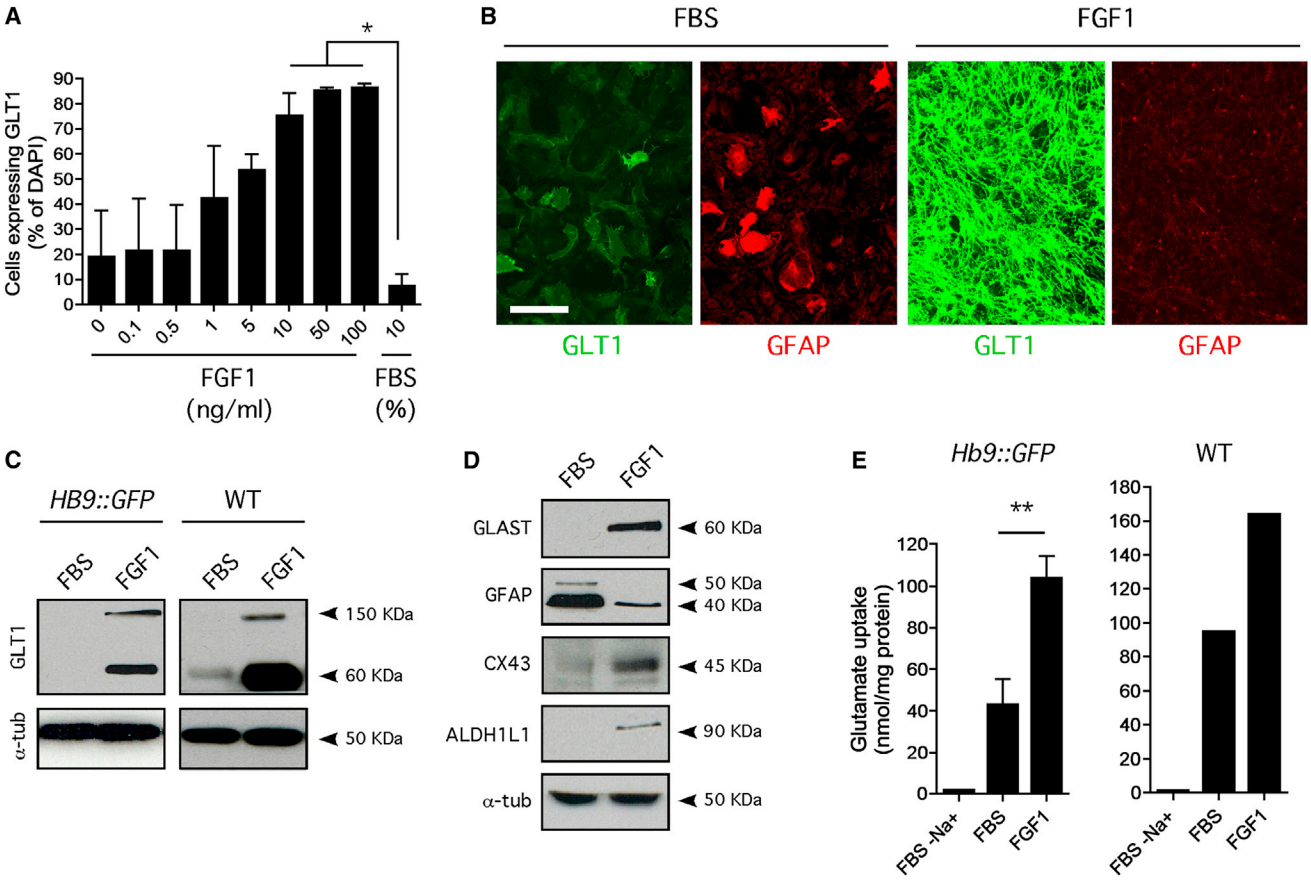

Figure 2. FGF1 Promotes Maturation of mESC-Derived Astrocytes

(A) Effects of increasing dose of FGF1 on the relative abundance of GLT1-expressing astrocytes in mESC-derived cultures (mean ± SEM for two independent experiments, three replicates per condition). One-way ANOVA reveals an effect of treatment above 5 ng/ml. $p = 0.013$; $F_{(8;9)} = 5.01$. The asterisk denotes $p < 0.05$.

(B) Compared to an FBS control (left), 50 ng/ml FGF1 (right) triggers a strong increase in GLT1 staining and a nearly complete loss of GFAP immunoreactivity. The scale bar represents 75 μm.

(C) Increased GLT1 expression following FGF1 treatment of astrocytes derived from two independent mESC lines (Hb9::GFP and wild-type) revealed by western blot analysis. Results are representative of three independent experiments. WT, wild-type.

(D) FGF1 is sufficient to induce appearance of GLAST, CX43, and ALDH1L1 but strongly decreases GFAP expression. Results are representative of three independent experiments.

(E) Na^+-dependent L-(^{3}H)-glutamate transport using two mESC lines differentiated into astrocytes shows an average 2-fold increase in uptake following treatment with FGF1 (bars show mean ± SEM; $n = 4$; $p = 0.0095$; $F_{(3;3)} = 1.286$. The double asterisks denote $p < 0.01$).

See also Figure S3.

(H13) and hiPSC (11a) lines. Neurons were initially abundant at early stages but disappeared over the period 30–60 DIV until, by 90 DIV, there were no neurons remaining (Figure 3C). Moreover, few CNPase-positive oligodendrocytes could be detected at either 40 or 90 DIV (<3% of total cells; Figure 3D), and whereas many cells at early stages expressed the neural crest marker p75, these too were spontaneously eliminated (data not shown). GFAP staining was first observed from 20–45 DIV, in the form of scattered $GFAP^+$ and $A2B5^+$ cells (Figure 3E; data not shown), whose long processes suggested they might be radial glia (Hirano and Goldman, 1988). Over the period 40–80 DIV, the abundance of multipolar GFAP-expressing cells with the $HoxB4^+/Otx2^-$ profile characteristic of spinal cord increased ~10-fold to >70% of DAPI-labeled cells (Figure 3F; data not shown), and by 80 DIV, astrocyte markers CD44, S100β, CX43, vimentin, NF1A, and aldolase C were all present in cultures from each of the four hESC/hiPSC lines (Figures 3G–3J). Nearly 100% of the cells expressed the glial marker S100β (Figure 3F), consistent with their homogeneous morphology (Figure S4).

We next analyzed the functional capacity of astrocytes derived following early neuralization. Excitatory amino-acid transporter 2 (EAAT2) (equivalent to rodent GLT1) was already detectable in a subset of cells (Figures 3I and 3J) and, accordingly, all human astrocyte cultures exhibited a basal level of Na^+-dependent glutamate transport (Figure 4A). Mechanical stimulation of single astrocytes from all four lines generated calcium waves that propagated to adjacent astrocytes (Figure 4B; data not shown). Lastly, the astrocytes expressed both brain-derived neurotrophic factor (BDNF) and glial-cell-line-derived neurotrophic factor (GDNF) and secreted factors that significantly enhanced survival

and neurite outgrowth from fluorescence-activated cell sorting (FACS)-purified human ESC-derived motor neurons (Figures 4C–4E). This correlates well with the growth-promoting activity of immature astrocytes reported in vivo (Filous et al., 2010; Goldshmit et al., 2012). Thus, early neuralization generates human spinal cord astrocytes expressing many canonical biochemical and functional traits.

Nevertheless, as with mESC cultures, maturation was less than complete and varied between lines. For example, the glial progenitor marker NF1A was strongly expressed in cultures from all four lines (Figure 3J). Moreover, even among mature markers, the populations derived from different stem cell lines were not homogeneous. For example, EAAT2 expression was consistently lower in the H13 hESC cultures, as shown by immunocytochemistry and western blotting (Figures 3I and 3J). We reasoned that this might reflect the absence of humoral maturation factors that astrocytes normally encounter in vivo. We therefore grafted 80- to 90-DIV hESC- and hiPSC-derived astrocytes into the striatum of adult rats (Figure 4F; Brederlau et al., 2006). After 2 and 7 weeks, staining for human nuclei in four animals per line transplanted revealed that grafted cells in all animals had survived (Figure S5). Survival in vivo is a characteristic of immature astrocytes (Filous et al., 2010) and, accordingly, at 7 weeks 86% ± 1% (mean ± SEM; n = 16; no significant differences between lines or time points) of grafted cells were $GFAP^+$ and 88% ± 6% expressed NF1A (Figure 4G). The presence of these immature markers demonstrated that the in vivo environment alone was not sufficient to induce quiescence and may have indeed stimulated astrocyte reactivity.

FGFs but Not TNFα Promote Maturation of Human Stem-Cell-Derived Astrocytes

We therefore tested candidate factors for their ability to promote maturation, focusing on FGF1 because of the potent effects we had found in the murine system. As a control, we used TNFα, because it has been implicated in triggering astrocytosis in neurodegenerative contexts (Cui et al., 2011) and was previously shown to activate primary human astrocytes in vitro (Croitoru-Lamoury et al., 2003; Meeuwsen et al., 2003). Human ESC and hiPSC lines were differentiated as above for 90 days and then thoroughly washed to remove any residual FBS. They were subsequently treated for 7 days with FBS (1% v/v), FGF1 (50 ng/ml), or TNFα (50 ng/ml), the latter two factors in the absence of serum. Although morphological changes were observed (Figure S4), levels of the canonical markers S100β and aldolase C were not affected by these treatments (Figures 5A and 5B), suggesting that the cells retained their astrocyte identity throughout. In striking contrast, western blotting revealed that FGF1 induced a nearly complete loss of expression of both GFAP and NF1A in both cell lines, whereas cells treated with TNFα showed little change in either marker (Figure 5B). Correspondingly, immunostaining for NF1A and GFAP was markedly reduced in the cell aggregates induced by FGF1 (Figures 5C and S6). To exclude the possibility that this might be a secondary effect of cell aggregation, we performed the same experiments after dissociation of cell clumps followed by replating. Similar reductions were observed (Figures S6A and S6B), confirming that these are direct effects of FGF. Another marker whose levels in human astrocytes were significantly reduced by FGF1 as compared to FBS was CX43 (Figure 5D). This is consistent with a more quiescent phenotype following FGF treatment (Theodoric et al., 2012). Although mESC-derived astrocytes treated with FGF showed the opposite change (Figure 2D), Cx43 levels in rodents rise during perinatal development (Dermietzel et al., 1989) and so this change may reflect developmental maturation. Overall, therefore, human astrocytes are induced to adopt a mature quiescent phenotype by FGF1 but not by TNFα.

To confirm this conclusion, we assayed functional changes triggered by each factor. Under pathophysiological conditions, reactive inflammatory astrocytes express low levels of glutamate transporters (Rothstein et al., 1995); this was potentially the case with our FBS cultures, which are rich in $GFAP^+$ astrocytes. In agreement with this, FGF1 led to a 2-fold increase in Na^+-dependent glutamate transport activity. Similar effects were seen with FGF2 (Figure S5E), whereas TNFα had no or even a negative effect (Figure 5E), as reported for primary astrocytes (Fine et al., 1996). Unexpectedly, given the increased transport, FGF1 induced no marked changes in EAAT2 protein or messenger RNA (mRNA) levels (Figures 5F and 5G). As an alternative explanation for the increased glutamate transport, we investigated EAAT1, a related transporter whose levels in gray-matter astrocytes in vivo also increase with postnatal age (Voutsinos-Porche et al., 2003a, 2003b). We indeed observed a 4-fold increase in *EAAT1* levels following treatment with FGF1, whereas TNFα had no effect (Figure 5H). Moreover, dihydrokainate (DHK) (an inhibitor of EAAT2 transport) had no effect on glutamate uptake (Figure S5F), further supporting the involvement of EAAT1. Moreover, similar effects of FGF were seen in aggregated or dissociated cultures, suggesting that the increased glutamate transport is not an indirect effect of cell clumping (Figure 5H). Overall, our results show that FGF1 or FGF2 but not TNFα are sufficient to induce a mature biochemical and functional phenotype in human, as in mouse, stem-cell-derived astrocytes.

TNFα and IL-1β, but Not FGF1, Trigger Reactivity of Human Pluripotent-Stem-Cell-Derived Astrocytes

Because TNFα had proven inactive in driving astrocyte maturation, we asked whether it was able to induce astrocyte activation. We monitored expression of the chemokines CXCL8 and RANTES (also known as IL8 and CCL5, respectively), which are strongly upregulated in human astrocyte primary cultures treated with TNFα (Croitoru-Lamoury et al., 2003; Meeuwsen et al., 2003), as well as expression of lipocalin-2 (LCN2) and tissue inhibitor of metalloproteinase-1 (TIMP1), which were recently shown to be upregulated in reactive astrocytes in vivo (Zamanian et al., 2012). Within 2 days of TNFα administration, levels of mRNA for CXCL8 and RANTES were increased >300-fold over those for cells maintained in FBS (Figure 6A), whereas 7 days after TNFα treatment, *LCN2* levels were also increased (>1,000-fold in R1 and 8-fold in 18c astrocytes; Figure 6B). Another proinflammatory cytokine, IL-1β, led to a 4,000-fold increase in *LCN2* (Figure S6F). In contrast, FGF1 induced a modest downregulation in both chemokines and LCN2 (Figures 6A and 6B). TIMP1 mRNA levels did not change more than 8-fold in any condition (data not shown), suggesting that it is less strongly regulated than LCN2 in cultured astrocytes. Thus,

Cell PRESS
Open ACCESS

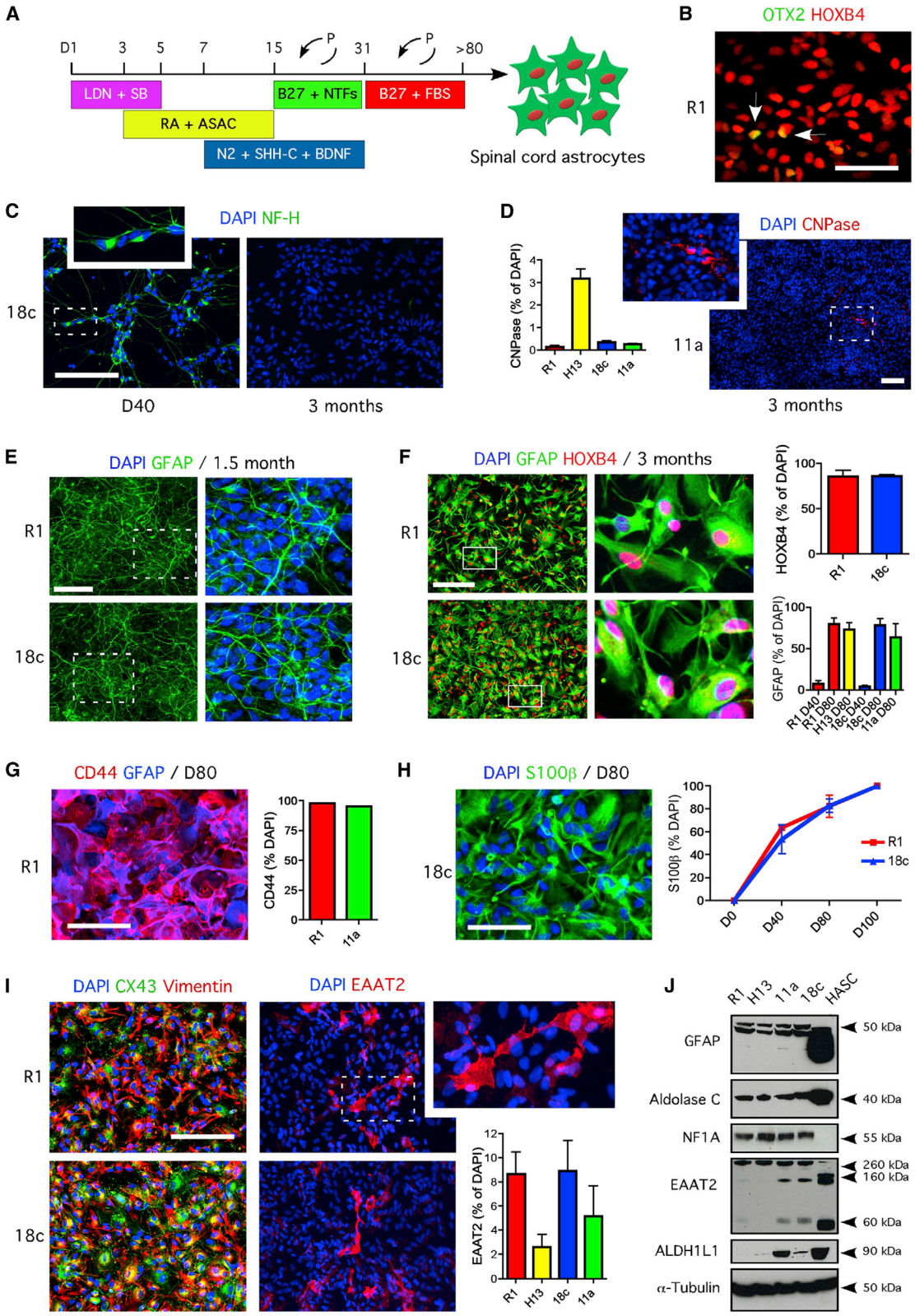

(legend on next page)

TNFα induces a molecular phenotype that is consistent with astrocyte reactivity.

To test this more directly, we measured the production of the cytokine IL-6, which in primary astrocytes acts in an autocrine manner to stimulate its own production (Van Wagoner et al., 1999). No IL-6 could be detected in FBS control cultures or in cells treated with FGF1 (Figure 6C). In marked contrast, TNFα led to an increase in IL-6 production that was already detectable after 1 day and increased to >300 pg/ml after 1 week (Figure 6C). Similarly strong responses to TNFα were observed in astrocytes generated from another hESC line (H13) and three other hiPSC lines (11a, 25b, and 39d; data not shown), and IL-1β produced similar effects (Figure S6). Therefore, both TNFα and IL-1β induce a reactive phenotype.

Overall, our data show that single factors can rapidly modify the phenotype of pluripotent-stem-cell-derived astrocytes in distinct and biologically relevant manners (Figures 6D and S6H).

DISCUSSION

The role of astrocytes in vivo varies widely according to their degree of developmental maturation or reactivity and potentially their regional specificity, yet the distinction between these functional states has not been clearly established in in vitro models. Having generated human spinal cord astrocytes from hESCs or hiPSCs through early neuralization, we focused on biochemical and functional characteristics that distinguish quiescence from reactivity in the animal and used them to define methods through which each state can be selectively enhanced in culture. Strikingly, we found that single factors were sufficient to promote such transitions: FGF1 or FGF2 are sufficient to strongly enhance maturation/quiescence without triggering inflammatory phenotypes, whereas TNFα or IL-1β produces the converse effect. Our data show clearly how exogenous factors can modify astrocyte functional status, and they provide a means of generating human patient-derived astrocytes that are functionally homogeneous for future studies of development or of disease.

One of the challenges in using human pluripotent stem cells for either basic or translational biology is the length and consequent variability of the protocols needed to generate specific cell types (Krencik and Zhang, 2011). One approach to the acceleration of protocols for astrocyte generation used in several recent publications is based on the initial generation of neural precursors, in some cases involving manual picking of rosettes (Emdad et al., 2012; Juopperi et al., 2012; Lafaille et al., 2012; Serio et al., 2013; Shaltouki et al., 2013). Given our interest in motor neuron biology and disease, we instead began by early neuralization of monolayer cultures followed by caudalization and ventralization, which we and others have shown to generate spinal neurons with high yield in shorter times (Amoroso et al., 2013; Boulting et al., 2011; Chambers et al., 2009). Our method allowed spinal cord astrocytes with the expected molecular and functional characteristics to be generated in half the time (80–90 days as compared to 180 days) needed for neurosphere-based approaches (Gupta and Kanungo, 2013; Krencik et al., 2011). However, as with all other protocols published to date, the astrocytes were immature, as judged by both marker expression and glutamate uptake as well as other traits, such as survival after transplantation.

We found that both FGF1 and FGF2 are capable of inducing a mature, quiescent astrocyte phenotype characterized by low GFAP and NF1A but high levels of glutamate transport. Our findings are distinct from other reported effects of FGFs in vitro but closely match developmental in vivo data. In vitro, FGFs have been reported to induce mitosis (Lin and Goldman, 2009) and gap junction coupling (Garré et al., 2010) but not maturation. Particularly striking are the divergent reports of responses to FGFs. Some studies report induction of stellate morphology (Cassina et al., 2005; Reilly et al., 1998) and even increased GFAP immunostaining (Cassina et al., 2005), whereas others observe dedifferentiation and adoption of a bipolar morphology (Goldshmit et al., 2012). It is likely that the different outcomes reflect the presence of different astrocyte subtypes or culture conditions. In vivo, FGFR3, which can be activated by both FGF1 and FGF2 (Chen and Hristova, 2011; Ornitz et al., 1996), is expressed specifically by astrocytes and their precursors in postnatal spinal cord (Pringle et al., 2003). Strikingly, in null mutant mice for FGFR3, there is a strong upregulation of GFAP

Figure 3. Rapid Generation of Spinal Cord Astrocytes from hESCs and hiPSCs following Early Neuralization

(A) Treatments used for efficient generation of hESC- and hiPSC-derived astrocytes. P, passage; LDN, LDN193189; SB, SB431542; ASAC, ascorbic acid; N2, N2 supplement; B27, B27 supplement; NTFs, neurotrophic factors (CNTF, BDNF, IGF-1, GDNF).

(B) Efficient conversion of human pluripotent stem cells—here shown for hESC (R1) line—into HOXB4$^+$ OTX2$^-$ spinal cord cultures. Representative of three independent experiments. The scale bar represents 50 μm.

(C) At 80 DIV, no neurofilament (NF-H)-expressing neurons are found in hESC- and hiPSC-derived cultures (here shown for line 18c). At 40 DIV, the fraction of NF-H-expressing cells was ~40% (data not shown). The scale bar represents 75 μm.

(D) At 80 DIV, very few CNPase-expressing oligodendrocytes are detected. Mean abundance ± SEM (n = 2–3 independent differentiations). The scale bar represents 50 μm.

(E) At 45 DIV, GFAP-expressing cells display bipolar morphology and resemble radial glia. The scale bar represents 50 μm.

(F) At 90 DIV, cultures are enriched in GFAP-expressing astrocytes, which retain their spinal cord identity, as revealed by HOXB4 expression (mean ± SEM; n = 3–4). The scale bar represents 50 μm.

(G) At 80 DIV, hESC- and hiPSC-derived cultures (here shown for R1) contain abundant astrocytes that express the canonical marker CD44 (mean ± SEM; n = 2). The scale bar represents 50 μm.

(H) The number of cells expressing the canonical astrocyte marker S100β increases over time to nearly 100% (mean ± SEM; n = 2–3). The scale bar represents 50 μm.

(I) At 80 DIV, hESC- and hiPSC-derived cultures (R1 and 18c) contain astrocytes that express canonical markers together with the EAAT2 transporter. Mean abundance ± SEM (n = 3–5 independent differentiations). The scale bar represents 75 μm.

(J) Western blotting confirms the expression of the astroglial markers in all lines tested. Human adult spinal cord (HASC) tissue was used as positive control. Blot representative of two independent experiments.

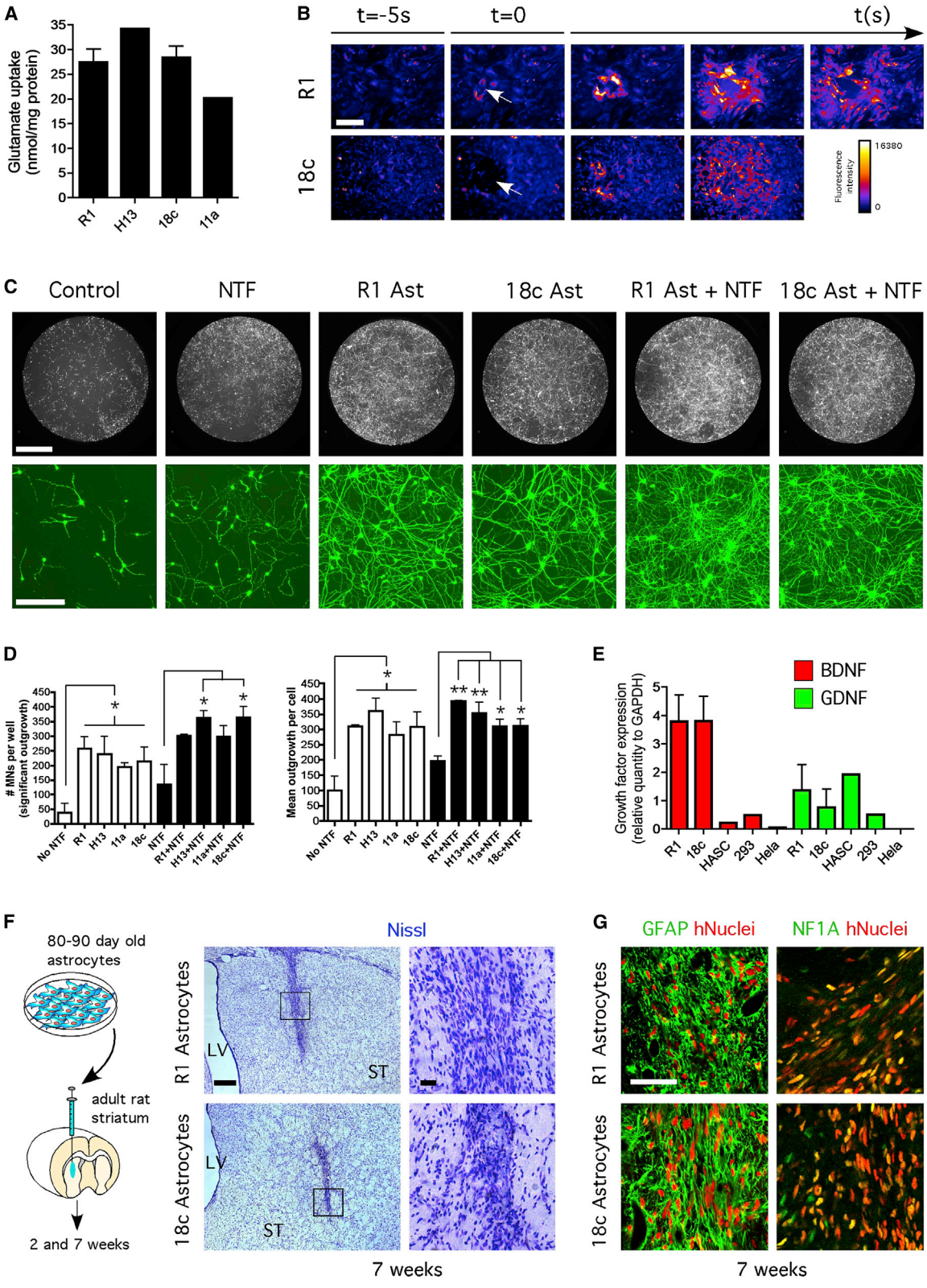

(legend on next page)

in spinal gray-matter from 2 months of age onward, and signaling through FGFR3 can repress GFAP (Pringle et al., 2003). In agreement with our findings, this suggests that FGFs drive and maintain a quiescent mature phenotype in vivo. In FGF2-null mutants, in apparent contrast, GFAP is reduced in spinal gray matter, but this was suggested by the authors to reflect an early developmental role for FGF2 (Irmady et al., 2011). Therefore, treatment of immature pluripotent stem-cell-derived astrocytes with FGF1/FGF2 is an effective and physiologically relevant means for inducing in vitro maturation.

Astroglial activation is associated with several nervous system pathologies (Glass et al., 2010). Focusing on motor neuron disease, specific astrocyte reactivity is observed in postmortem cortex and spinal cord of ALS patients (Kamo et al., 1987; Murayama et al., 1991; Schiffer et al., 1996) and inflammatory gene expression is upregulated in astrocytes derived from sporadic ALS patients (Haidet-Phillips et al., 2011). GFAP and ALDH1L1 are upregulated following injury and in the ALS spinal cord (Anthony and Heintz, 2007; Yang et al., 2011), and a dramatic loss of GLT1 is observed in other pathological situations (Chao et al., 2010; Faideau et al., 2010; Rothstein et al., 1995). For reliable disease modeling, it is therefore essential to reproduce the reactive state. We found that TNFα induces, in human stem-cell-derived astrocytes, a phenotype characterized by high GFAP and production of inflammatory chemokines and cytokines, as well as very strong upregulation of *Lcn2,* the top gene in the list of markers shown by Zamanian et al. (2012) to be upregulated in two different models of reactivity. This is of particular interest, because Lcn2 was recently reported to trigger neuronal death and to contribute to astrocyte toxicity (Bi et al., 2013). In parallel experiments, we extensively tested the effects of other potential activators. For example, IL-1β elicited several characteristic signatures of activation but also promoted GLAST expression, a marker of maturation (data not shown). Opposite effects of TNFα and IL-1β on astrocytes have previously been reported (Sokolova et al., 2012). We therefore recommend, for standard differentiations, the use of the more selective activator TNFα.

The two populations of astrocytes we have generated will have multiple uses. We report that human stem-cell-derived astrocytes are capable of an immunological response similar to that evoked by cytokines in primary human astrocytes (Meeuwsen et al., 2003), and this should be important for modeling human pathological processes in vitro. Mature, quiescent astrocytes will clearly be important for studying normal function but may also be relevant to disease conditions. In vitro, astrocytes from mutant superoxide dismutase 1 (SOD1) mouse models of ALS release toxic factors for motor neurons (Di Giorgio et al., 2007; Nagai et al., 2007). Accordingly, in vivo, reduction of SOD1 levels in GFAP$^+$ (and therefore reactive) cells leads to an increase in survival of the mice (Yamanaka et al., 2008). This might suggest that the reactive, GFAP$^+$ astrocytes are the principal contributors to toxicity for motor neurons. However, astrocytes lacking SOD1 retained GFAP expression, although they were less toxic (Yamanaka et al., 2008). Therefore, astrocyte toxicity and reactivity can be uncoupled. Thus, in assaying the contribution of astrocytes to pathology in vivo, it is critical to evaluate even mature, quiescent populations. Moreover, for modeling neurodegenerative disease in vitro, it will be essential to distinguish between the effects of mature and activated astrocytes, and our protocol provides a means of doing this using both rodent and human cells.

EXPERIMENTAL PROCEDURES

Differentiation of Spinal Cord Astrocytes from Mouse and Human Pluripotent Stem Cells

Rodent motor neuron cultures were dissociated into single-cell suspension and grown in neurosphere (NS) medium supplemented with FGF2 and epidermal growth factor. Neurospheres were dissociated, and single cells were seeded onto 100 μg/ml poly-L-ornithine and 15 μg/ml laminin-coated surfaces in NS medium supplemented with 10% FBS. Neuralized human motor neuron cultures (aged 31 DIV) were passaged onto 100 μg/ml polyornithine and 3–5 μg/ml laminin-coated surfaces in NS medium supplemented with 1% FBS. Rodent and human cultures were passaged when they reached confluency. The presence of astrocytes was detected by immunocytochemistry. All human iPSC lines were derived from anonymized human skin biopsies following approval by the Columbia University Institutional Review Board.

RNA Isolation and Quantitative PCR

The total RNA was isolated from cultured cells with RNeasy Kit (QIAGEN). Complementary DNA (cDNA) was generated using the Verso TM cDNA Kit and was used as template for the quantitative PCR (qPCR).

Measurement of Glutamate Uptake

Cells were incubated for 5 min at 37°C in Na^+ buffer containing 0.5 μM L-glutamate and 0.3 μCi L-[^{3}H]-glutamate per sample. Cells were then lysed with 0.1N

Figure 4. Human Stem-Cell-Derived Astrocytes Are Functional but Not Completely Mature

(A) All hESC- and hiPSC-derived astrocytes show Na^+-dependent L-(^{3}H)-glutamate transport activity (SEM shown for n = 3 independent experiments were performed).

(B) Mechanical stimulation (white arrow) of a single astrocyte induces a wave of calcium influx that propagates to adjacent astrocytes. The scale bar represents 75 μm.

(C) Whole-well imaging of hESC-derived motor neurons live-stained with calcein following coculture with astrocytes in the presence or not of exogenous growth factors (NTF). Green images show selected fields. The scale bars represent 200 μm (top) and 75 μm (bottom).

(D) Human astrocytes enhance survival and growth of hESC-derived motor neurons following coculture. One-way ANOVA reveals an effect of treatment. For motor neuron survival, *P* and F values are: no NTF versus astrocyte coculture: p = 0.0224, $F_{(4;8)}$ = 5.25 and NTF versus astrocyte coculture supplemented with NTF: p = 0.0239, $F_{(4;9)}$ = 4.79. For neurite outgrowth, *P* and F values are: no NTF versus astrocyte coculture: p = 0.0221, $F_{(4;8)}$ = 5.38 and NTF versus astrocyte supplemented with NTF coculture: p = 0.0045, $F_{(4;9)}$ = 8.19. The asterisk denotes $p < 0.01$ and double asterisks denote $p < 0.001$, which denote statistically significant differences.

(E) qPCR analysis shows that hESC- and hiPSC-derived astrocytes express BDNF and GDNF at levels comparable to or greater than HASC tissue. Error bars indicate SEM for n = 3 independent experiments (all in duplicate).

(F) hESC- and hiPSC-derived astrocytes do not form teratomas in the striatum of adult rats, even at 7 weeks posttransplantation, revealed by Nissl staining. The scale bars represent 250 μm and 50 μm.

(G) Even at 7 weeks posttransplantation, human ESC- and hiPSC-derived astrocytes maintain an immature/reactive phenotype. The scale bar represents 50 μm. See also Figures S4 and S5.

Cell PRESS
Open ACCESS

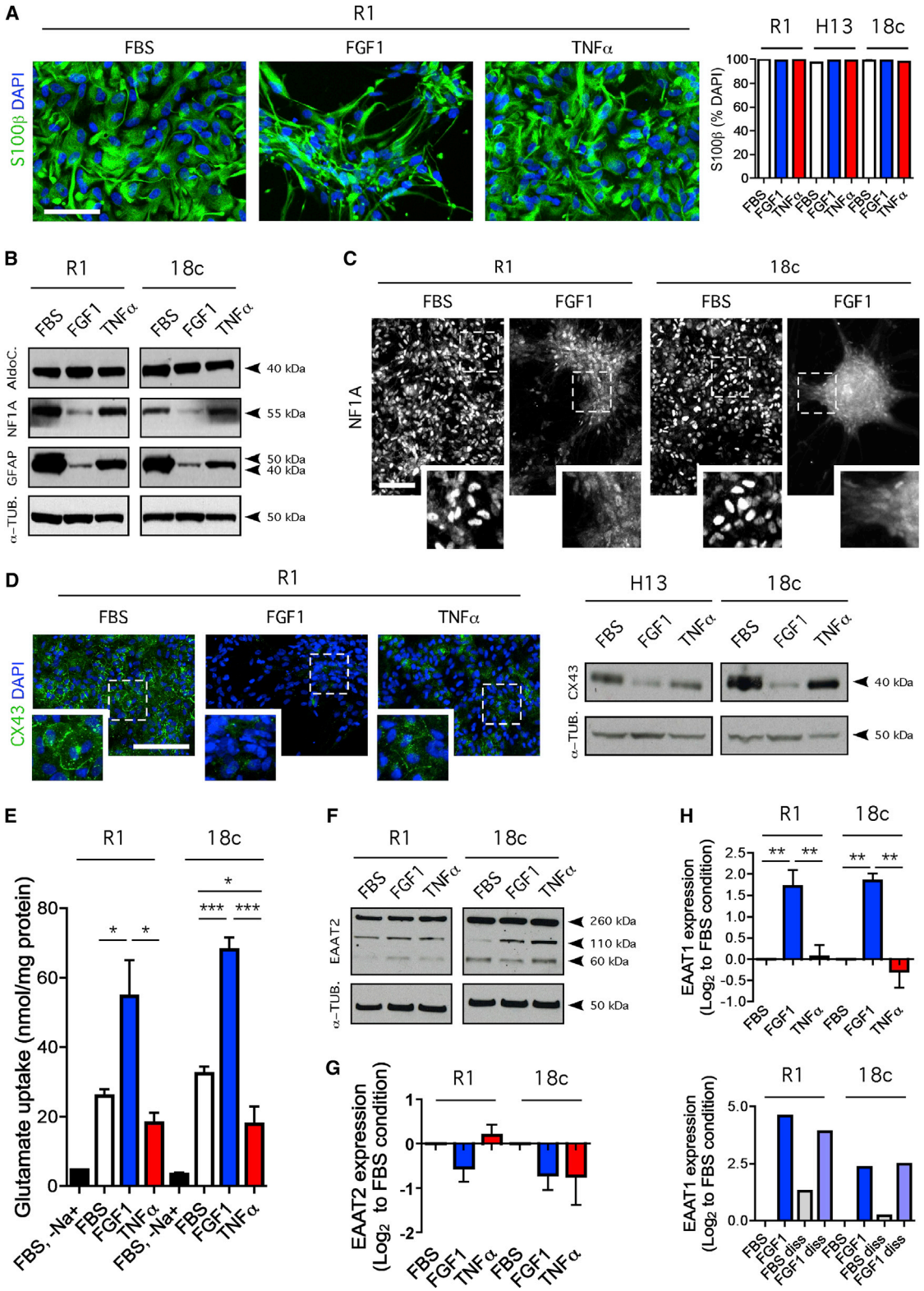

Figure 5. FGF but Not TNFα Triggers Biochemical and Functional Maturation of Human Stem-Cell-Derived Astrocytes

(A) Astroglial purity at 90 DIV; virtually all cells express S100β in all conditions. The scale bar represents 50 μm.

(B) Dramatic reduction in GFAP and NF1A protein levels but not aldolase C following treatment with FGF1 at 80 DIV, whereas TNFα has little impact. α-tubulin was used as loading control. Results are typical of three independent experiments.

(legend continued on next page)

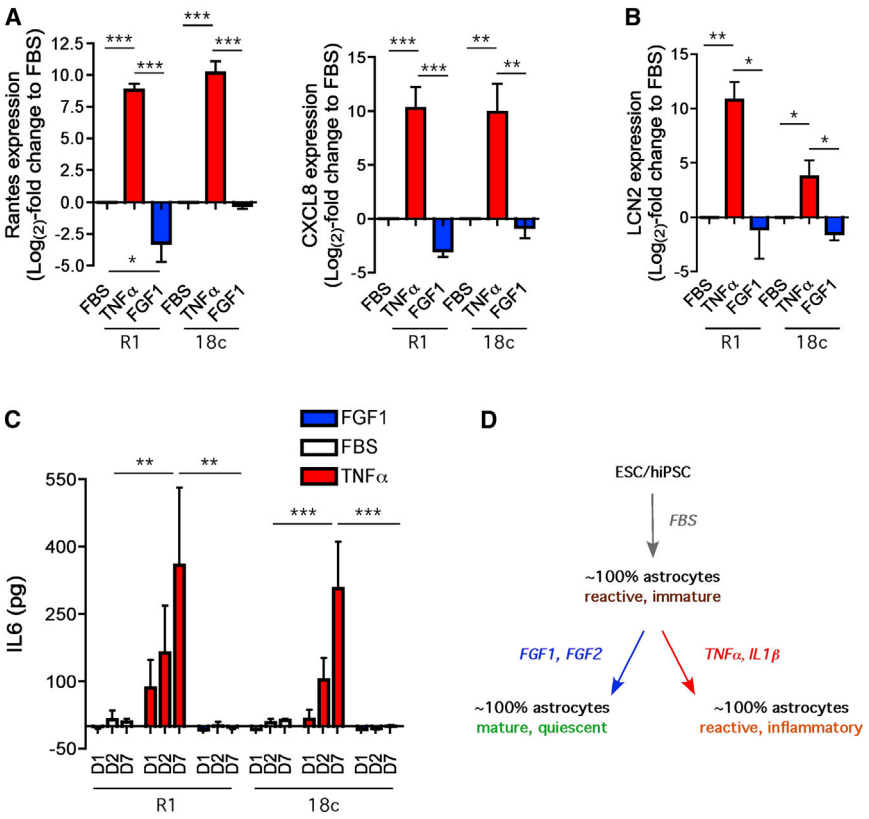

Figure 6. TNFα but Not FGF1 Triggers Reactivity of hESC- and hiPSC-Derived Astrocytes

(A) Strong effects of TNFα but not FGF1 on RANTES and CXCL8 expression (mean ± SEM; n = 4 for R1 and n = 3 for 18c). One-way ANOVA reveals an effect of treatment. *P* and F values are: RANTES R1: p = 0.0002, F(2;6) = 46.99; RANTES 18c: p < 0.0001, F(2;6) = 111.7; CXCL8 R1: p = 0.0006, F(2;6) = 32.73; and CXCL8 18c: p < 0.006, F(2;6) = 13.03. The asterisk denotes p < 0.05, double asterisks denote p < 0.001, and triple asterisks denote p < 0.0001, which denote statistically significant differences between treatments.

(B) hESC- and hiPSC-derived astrocytes strongly express LCN2 after 7 days treatment with TNFα but not with FGF1 (mean ± SEM; n = 3). One-way ANOVA reveals an effect of treatment. *P* and F values are: R1: p = 0.0076, $F_{(2;6)}$ = 12.26 and 18c: p < 0.02, $F_{(2;6)}$ = 8.06. The asterisk denotes p < 0.05 and double asterisks denote p < 0.001, which denote statistically significant differences between treatments.

(C) TNFα but not FGF1 triggers IL6 release over time. Two-way ANOVA reveals an effect of treatment for R1 line and treatment and time for 18c line. *P* and F values are: IL-6 R1 (treatment): p = 0.0035, $F_{(2;18)}$ = 7.88; IL-6 18c (treatment): p = 0.0003, $F_{(2;18)}$ = 111.7; and IL-6 18c (time): p = 0.01, $F_{(2;18)}$ = 5.86. The double asterisks denote p < 0.001 and triple asterisks denote p < 0.0001, which denote statistically significant differences between treatments on day 7.

(D) hESC- and hiPSC-derived astrocytes have an immature reactive phenotype when cultured in FBS but can be triggered by single factors to adopt a mature, quiescent phenotype (FGF1 or FGF2) or a reactive inflammatory one (TNFα or IL-1β).

See also Figure S6.

NaOH solution, and radioactivity was measured using a scintillation counter. Radioactive counts were normalized to total protein per culture well.

IL-6 ELISA

Astrocytes were treated for 1, 2, or 7 days with medium containing FBS, FGF1, IL-1β, and TNFα. Medium was then harvested and used for the human IL-6 ELISA assay following manufacturer's instructions (Invitrogen). Absorbance was measured at 450 nm.

Statistical Analyses

For each independent experiment, duplicate sometimes triplicate cultures were analyzed from twelve 10X fields per sample. All quantitative data were analyzed using Prism 5.0c (GraphPad). Sample groups were subjected to one- or two-way ANOVA, with Newman-Keuls post hoc comparison when all conditions are compared to each other and Dunnett posthoc comparison when all columns are compared to control condition (e.g., FBS treatment). The null hypothesis was rejected at 0.05 for all ANOVAs and post hoc tests.

See the Extended Experimental Procedures for more information.

SUPPLEMENTAL INFORMATION

Supplemental Information includes Extended Results, Extended Experimental Procedures, and six figures and can be found with this article online at http://dx.doi.org/10.1016/j.celrep.2013.06.021.

(C) Reduced abundance of NF1A-expressing cells in 80-day hESC- and hiPSC-derived astrocytes following treatment for 7 days with FGF1 (50 ng/ml). FGF1 leads to cell aggregation. The scale bar represents 50 μm.

(D) Decrease in CX43 expression following treatment with FGF1 as compared to TNFα. Results are typical of two independent experiments. The scale bar represents 75 μm.

(E) Two-fold increase in glutamate uptake in astrocytes treated with FGF1 but not TNFα. For line 18c, one-way ANOVA (p < 0.0001; $F_{(2;12)}$ = 48.58; n = 5) followed by Newman-Keuls multiple comparison posthoc test shows FGF1 treatment significantly (***p < 0.0001) promotes uptake over control- (FBS) and TNFα-treated cultures. TNFα treatment decreases uptake (*p < 0.05). Similar results were obtained for line R1.

(F) Absence of pronounced change in EAAT2 protein levels following FGF1 or TNFα treatment. Results are typical of four independent experiments.

(G) qPCR analysis shows no major change in EAAT2 levels when astrocytes are cultured with FGF1 and TNFα.

(H) qPCR analysis shows that hESC- and hiPSC-derived astrocytes strongly upregulate the alternative glutamate transporter EAAT1 7 days after treatment with FGF1 but not TNFα (mean ± SEM; n = 4 for R1 and n = 3 for 18c). One-way ANOVA reveals an effect of treatment. *P* and F values are: R1: p = 0.0028, $F_{(2;9)}$ = 12.18 and 18c: p = 0.0019, $F_{(2;6)}$ = 21.94. The double asterisks denote p < 0.001, which denotes statistically significant difference between treatments. Bottom panel: Similar changes are observed after replating of dissociated clumps (n = 1 for R1 and 18c).

See also Figures S4 and S5.

ACKNOWLEDGMENTS

We thank M.W. Amoroso and G.F. Croft (Project A.L.S. Laboratory) for sharing data on pilot astrocyte differentiations using noggin, D.H. Oakley for advice on calcium imaging, and B.E. Lewis for help with cell culture and western blotting. H. Hua provided valuable input on qPCR reagents, and the Eggan Laboratory (Harvard Stem Cell Institute) and H. Mitsumoto, J. Montes, P. Kaufmann, and J. Andrews (Columbia) collaborated to generate hiPSCs. We thank J. Goldman for critical reading of the manuscript and N. Maragakis, J. Goldman, M. Rao, B. Barres, members of all our labs and the investigators of the P^2ALS consortium, as well as Valerie and Meredith Estess for many helpful discussions. This work was funded by Project A.L.S. and P^2ALS. L.R. was supported by Project A.L.S., the Dr. Leigh G. Cascarilla Post-Doctoral Fellowships in Stem Cell Research, and the Swedish Brain Foundation/Hjärnfonden. N.J.L. was supported by the Portuguese Foundation for Science and Technology SFRH/BD/33421/2008 and the Luso-American Development Foundation. S.P. and V.J.L. were funded through NINDS R01 NS042269-05A2. S.P. is the recipient of the Page and William Black professorship, and C.E.H. is the Gurewitsch/Vidda Professor of Regenerative Medicine.

L.R. performed experiments and analysis. N.J.L. performed motor neuron differentiation and FACS and assisted with survival studies and cell culture. A.D.G. assisted with cell culture and western blots and performed ELISA. E.J.Y. and R.S. performed glutamate uptake assays. V.J.L. assisted with transplantations and immunosuppression. Y.A.K. and C.A.K. assisted with cell culture, RT-PCR, and qPCR. J.D.R. and S.P. provided reagents and input on experiments. L.R., H.W., and C.E.H. conceived the experiments and wrote the manuscript.

Received: July 31, 2012
Revised: May 15, 2013
Accepted: June 18, 2013
Published: August 29, 2013

REFERENCES

Abbott, N.J. (1988). Developmental neurobiology. The milieu is the message. Nature *332*, 490–491.

Allaman, I., Bélanger, M., and Magistretti, P.J. (2011). Astrocyte-neuron metabolic relationships: for better and for worse. Trends Neurosci. *34*, 76–87.

Amoroso, M.W., Croft, G.F., Williams, D.J., O'Keeffe, S., Carrasco, M.A., Davis, A.R., Roybon, L., Oakley, D.H., Maniatis, T., Henderson, C.E., and Wichterle, H. (2013). Accelerated high-yield generation of limb-innervating motor neurons from human stem cells. J. Neurosci. *33*, 574–586.

Anthony, T.E., and Heintz, N. (2007). The folate metabolic enzyme ALDH1L1 is restricted to the midline of the early CNS, suggesting a role in human neural tube defects. J. Comp. Neurol. *500*, 368–383.

Bernardinelli, Y., Salmon, C., Jones, E.V., Farmer, W.T., Stellwagen, D., and Murai, K.K. (2011). Astrocytes display complex and localized calcium responses to single-neuron stimulation in the hippocampus. J. Neurosci. *31*, 8905–8919.

Bi, F., Huang, C., Tong, J., Qiu, G., Huang, B., Wu, Q., Li, F., Xu, Z., Bowser, R., Xia, X.G., and Zhou, H. (2013). Reactive astrocytes secrete lcn2 to promote neuron death. Proc. Natl. Acad. Sci. USA *110*, 4069–4074.

Bock, C., Kiskinis, E., Verstappen, G., Gu, H., Boulting, G., Smith, Z.D., Ziller, M., Croft, G.F., Amoroso, M.W., Oakley, D.H., et al. (2011). Reference Maps of human ES and iPS cell variation enable high-throughput characterization of pluripotent cell lines. Cell *144*, 439–452.

Boulting, G.L., Kiskinis, E., Croft, G.F., Amoroso, M.W., Oakley, D.H., Wainger, B.J., Williams, D.J., Kahler, D.J., Yamaki, M., Davidow, L., et al. (2011). A functionally characterized test set of human induced pluripotent stem cells. Nat. Biotechnol. *29*, 279–286.

Brederlau, A., Correia, A.S., Anisimov, S.V., Elmi, M., Paul, G., Roybon, L., Morizane, A., Bergquist, F., Riebe, I., Nannmark, U., et al. (2006). Transplantation of human embryonic stem cell-derived cells to a rat model of Parkinson's disease: effect of in vitro differentiation on graft survival and teratoma formation. Stem Cells *24*, 1433–1440.

Caldwell, M.A., He, X., Wilkie, N., Pollack, S., Marshall, G., Wafford, K.A., and Svendsen, C.N. (2001). Growth factors regulate the survival and fate of cells derived from human neurospheres. Nat. Biotechnol. *19*, 475–479.

Cassina, P., Pehar, M., Vargas, M.R., Castellanos, R., Barbeito, A.G., Estévez, A.G., Thompson, J.A., Beckman, J.S., and Barbeito, L. (2005). Astrocyte activation by fibroblast growth factor-1 and motor neuron apoptosis: implications for amyotrophic lateral sclerosis. J. Neurochem. *93*, 38–46.

Chambers, S.M., Fasano, C.A., Papapetrou, E.P., Tomishima, M., Sadelain, M., and Studer, L. (2009). Highly efficient neural conversion of human ES and iPS cells by dual inhibition of SMAD signaling. Nat. Biotechnol. *27*, 275–280.

Chao, X.D., Fei, F., and Fei, Z. (2010). The role of excitatory amino acid transporters in cerebral ischemia. Neurochem. Res. *35*, 1224–1230.

Chen, F., and Hristova, K. (2011). The physical basis of FGFR3 response to fgf1 and fgf2. Biochemistry *50*, 8576–8582.

Croitoru-Lamoury, J., Guillemin, G.J., Boussin, F.D., Mognetti, B., Gigout, L.I., Chéret, A., Vaslin, B., Le Grand, R., Brew, B.J., and Dormont, D. (2003). Expression of chemokines and their receptors in human and simian astrocytes: evidence for a central role of TNF alpha and IFN gamma in CXCR4 and CCR5 modulation. Glia *41*, 354–370.

Cui, M., Huang, Y., Tian, C., Zhao, Y., and Zheng, J. (2011). FOXO3a inhibits TNF-α- and IL-1β-induced astrocyte proliferation:Implication for reactive astrogliosis. Glia *59*, 641–654.

Dermietzel, R., Traub, O., Hwang, T.K., Beyer, E., Bennett, M.V., Spray, D.C., and Willecke, K. (1989). Differential expression of three gap junction proteins in developing and mature brain tissues. Proc. Natl. Acad. Sci. USA *86*, 10148–10152.

Di Giorgio, F.P., Carrasco, M.A., Siao, M.C., Maniatis, T., and Eggan, K. (2007). Non-cell autonomous effect of glia on motor neurons in an embryonic stem cell-based ALS model. Nat. Neurosci. *10*, 608–614.

Elde, R., Cao, Y.H., Cintra, A., Brelje, T.C., Pelto-Huikko, M., Junttila, T., Fuxe, K., Pettersson, R.F., and Hökfelt, T. (1991). Prominent expression of acidic fibroblast growth factor in motor and sensory neurons. Neuron *7*, 349–364.

Emdad, L., D'Souza, S.L., Kothari, H.P., Qadeer, Z.A., and Germano, I.M. (2012). Efficient differentiation of human embryonic and induced pluripotent stem cells into functional astrocytes. Stem Cells Dev. *21*, 404–410.

Faideau, M., Kim, J., Cormier, K., Gilmore, R., Welch, M., Auregan, G., Dufour, N., Guillermier, M., Brouillet, E., Hantraye, P., et al. (2010). In vivo expression of polyglutamine-expanded huntingtin by mouse striatal astrocytes impairs glutamate transport: a correlation with Huntington's disease subjects. Hum. Mol. Genet. *19*, 3053–3067.

Filous, A.R., Miller, J.H., Coulson-Thomas, Y.M., Horn, K.P., Alilain, W.J., and Silver, J. (2010). Immature astrocytes promote CNS axonal regeneration when combined with chondroitinase ABC. Dev. Neurobiol. *70*, 826–841.

Fine, S.M., Angel, R.A., Perry, S.W., Epstein, L.G., Rothstein, J.D., Dewhurst, S., and Gelbard, H.A. (1996). Tumor necrosis factor alpha inhibits glutamate uptake by primary human astrocytes. Implications for pathogenesis of HIV-1 dementia. J. Biol. Chem. *271*, 15303–15306.

Garré, J.M., Retamal, M.A., Cassina, P., Barbeito, L., Bukauskas, F.F., Sáez, J.C., Bennett, M.V., and Abudara, V. (2010). FGF-1 induces ATP release from spinal astrocytes in culture and opens pannexin and connexin hemichannels. Proc. Natl. Acad. Sci. USA *107*, 22659–22664.

Glass, C.K., Saijo, K., Winner, B., Marchetto, M.C., and Gage, F.H. (2010). Mechanisms underlying inflammation in neurodegeneration. Cell *140*, 918–934.

Goldshmit, Y., Sztal, T.E., Jusuf, P.R., Hall, T.E., Nguyen-Chi, M., and Currie, P.D. (2012). Fgf-dependent glial cell bridges facilitate spinal cord regeneration in zebrafish. J. Neurosci. *32*, 7477–7492.

Gupta, R.K., and Kanungo, M. (2013). Glial molecular alterations with mouse brain development and aging: up-regulation of the Kir4.1 and aquaporin-4. Age (Dordr) *35*, 59–67.

Gwak, Y.S., Kang, J., Unabia, G.C., and Hulsebosch, C.E. (2012). Spatial and temporal activation of spinal glial cells: role of gliopathy in central neuropathic pain following spinal cord injury in rats. Exp. Neurol. *234*, 362–372.

Haidet-Phillips, A.M., Hester, M.E., Miranda, C.J., Meyer, K., Braun, L., Frakes, A., Song, S., Likhite, S., Murtha, M.J., Foust, K.D., et al. (2011). Astrocytes from familial and sporadic ALS patients are toxic to motor neurons. Nat. Biotechnol. *29*, 824–828.

Hirano, M., and Goldman, J.E. (1988). Gliogenesis in rat spinal cord: evidence for origin of astrocytes and oligodendrocytes from radial precursors. J. Neurosci. Res. *21*, 155–167.

Hu, B.Y., Weick, J.P., Yu, J., Ma, L.X., Zhang, X.Q., Thomson, J.A., and Zhang, S.C. (2010). Neural differentiation of human induced pluripotent stem cells follows developmental principles but with variable potency. Proc. Natl. Acad. Sci. USA *107*, 4335–4340.

Huang, Y.H., and Bergles, D.E. (2004). Glutamate transporters bring competition to the synapse. Curr. Opin. Neurobiol. *14*, 346–352.

Imura, T., Nakano, I., Kornblum, H.I., and Sofroniew, M.V. (2006). Phenotypic and functional heterogeneity of GFAP-expressing cells in vitro: differential expression of LeX/CD15 by GFAP-expressing multipotent neural stem cells and non-neurogenic astrocytes. Glia *53*, 277–293.

Irmady, K., Zechel, S., and Unsicker, K. (2011). Fibroblast growth factor 2 regulates astrocyte differentiation in a region-specific manner in the hindbrain. Glia *59*, 708–719.

James, D., Noggle, S.A., Swigut, T., and Brivanlou, A.H. (2006). Contribution of human embryonic stem cells to mouse blastocysts. Dev. Biol. *295*, 90–102.

Juopperi, T.A., Kim, W.R., Chiang, C.H., Yu, H., Margolis, R.L., Ross, C.A., Ming, G.L., and Song, H. (2012). Astrocytes generated from patient induced pluripotent stem cells recapitulate features of Huntington's disease patient cells. Mol. Brain *5*, 17.

Kamo, H., Haebara, H., Akiguchi, I., Kameyama, M., Kimura, H., and McGeer, P.L. (1987). A distinctive distribution of reactive astroglia in the precentral cortex in amyotrophic lateral sclerosis. Acta Neuropathol. *74*, 33–38.

Karumbayaram, S., Novitch, B.G., Patterson, M., Umbach, J.A., Richter, L., Lindgren, A., Conway, A.E., Clark, A.T., Goldman, S.A., Plath, K., et al. (2009). Directed differentiation of human-induced pluripotent stem cells generates active motor neurons. Stem Cells *27*, 806–811.

Krencik, R., and Zhang, S.C. (2011). Directed differentiation of functional astroglial subtypes from human pluripotent stem cells. Nat. Protoc. *6*, 1710–1717.

Krencik, R., Weick, J.P., Liu, Y., Zhang, Z.J., and Zhang, S.C. (2011). Specification of transplantable astroglial subtypes from human pluripotent stem cells. Nat. Biotechnol. *29*, 528–534.

Kriks, S., Shim, J.W., Piao, J., Ganat, Y.M., Wakeman, D.R., Xie, Z., Carrillo-Reid, L., Auyeung, G., Antonacci, C., Buch, A., et al. (2011). Dopamine neurons derived from human ES cells efficiently engraft in animal models of Parkinson's disease. Nature *480*, 547–551.

Kuegler, P.B., Baumann, B.A., Zimmer, B., Keller, S., Marx, A., Kadereit, S., and Leist, M. (2012). GFAP-independent inflammatory competence and trophic functions of astrocytes generated from murine embryonic stem cells. Glia *60*, 218–228.

Lafaille, F.G., Pessach, I.M., Zhang, S.Y., Ciancanelli, M.J., Herman, M., Abhyankar, A., Ying, S.W., Keros, S., Goldstein, P.A., Mostoslavsky, G., et al. (2012). Impaired intrinsic immunity to HSV-1 in human iPSC-derived TLR3-deficient CNS cells. Nature *491*, 769–773.

Lee, S.C., Liu, W., Dickson, D.W., Brosnan, C.F., and Berman, J.W. (1993). Cytokine production by human fetal microglia and astrocytes. Differential induction by lipopolysaccharide and IL-1 beta. J. Immunol. *150*, 2659–2667.

Li, X.J., Du, Z.W., Zarnowska, E.D., Pankratz, M., Hansen, L.O., Pearce, R.A., and Zhang, S.C. (2005). Specification of motoneurons from human embryonic stem cells. Nat. Biotechnol. *23*, 215–221.

Lie, D.C., Colamarino, S.A., Song, H.J., Désiré, L., Mira, H., Consiglio, A., Lein, E.S., Jessberger, S., Lansford, H., Dearie, A.R., and Gage, F.H. (2005). Wnt signalling regulates adult hippocampal neurogenesis. Nature *437*, 1370–1375.

Lin, G., and Goldman, J.E. (2009). An FGF-responsive astrocyte precursor isolated from the neonatal forebrain. Glia *57*, 592–603.

McCarthy, K.D., and de Vellis, J. (1980). Preparation of separate astroglial and oligodendroglial cell cultures from rat cerebral tissue. J. Cell Biol. *85*, 890–902.

Meeuwsen, S., Persoon-Deen, C., Bsibsi, M., Ravid, R., and van Noort, J.M. (2003). Cytokine, chemokine and growth factor gene profiling of cultured human astrocytes after exposure to proinflammatory stimuli. Glia *43*, 243–253.

Mitani, A., and Tanaka, K. (2003). Functional changes of glial glutamate transporter GLT-1 during ischemia: an in vivo study in the hippocampal CA1 of normal mice and mutant mice lacking GLT-1. J. Neurosci. *23*, 7176–7182.

Morrow, T., Song, M.R., and Ghosh, A. (2001). Sequential specification of neurons and glia by developmentally regulated extracellular factors. Development *128*, 3585–3594.

Murayama, S., Inoue, K., Kawakami, H., Bouldin, T.W., and Suzuki, K. (1991). A unique pattern of astrocytosis in the primary motor area in amyotrophic lateral sclerosis. Acta Neuropathol. *82*, 456–461.

Nagai, M., Re, D.B., Nagata, T., Chalazonitis, A., Jessell, T.M., Wichterle, H., and Przedborski, S. (2007). Astrocytes expressing ALS-linked mutated SOD1 release factors selectively toxic to motor neurons. Nat. Neurosci. *10*, 615–622.

Okamoto, M., Inoue, K., Iwamura, H., Terashima, K., Soya, H., Asashima, M., and Kuwabara, T. (2011). Reduction in paracrine Wnt3 factors during aging causes impaired adult neurogenesis. FASEB J. *25*, 3570–3582.

Ornitz, D.M., Xu, J., Colvin, J.S., McEwen, D.G., MacArthur, C.A., Coulier, F., Gao, G., and Goldfarb, M. (1996). Receptor specificity of the fibroblast growth factor family. J. Biol. Chem. *271*, 15292–15297.

Panatier, A., Vallée, J., Haber, M., Murai, K.K., Lacaille, J.C., and Robitaille, R. (2011). Astrocytes are endogenous regulators of basal transmission at central synapses. Cell *146*, 785–798.

Pringle, N.P., Yu, W.P., Howell, M., Colvin, J.S., Ornitz, D.M., and Richardson, W.D. (2003). Fgfr3 expression by astrocytes and their precursors: evidence that astrocytes and oligodendrocytes originate in distinct neuroepithelial domains. Development *130*, 93–102.

Reilly, J.F., Maher, P.A., and Kumari, V.G. (1998). Regulation of astrocyte GFAP expression by TGF-beta1 and FGF-2. Glia *22*, 202–210.

Rothstein, J.D., Van Kammen, M., Levey, A.I., Martin, L.J., and Kuncl, R.W. (1995). Selective loss of glial glutamate transporter GLT-1 in amyotrophic lateral sclerosis. Ann. Neurol. *38*, 73–84.

Rothstein, J.D., Dykes-Hoberg, M., Pardo, C.A., Bristol, L.A., Jin, L., Kuncl, R.W., Kanai, Y., Hediger, M.A., Wang, Y., Schielke, J.P., and Welty, D.F. (1996). Knockout of glutamate transporters reveals a major role for astroglial transport in excitotoxicity and clearance of glutamate. Neuron *16*, 675–686.

Schiffer, D., Cordera, S., Cavalla, P., and Migheli, A. (1996). Reactive astrogliosis of the spinal cord in amyotrophic lateral sclerosis. J. Neurol. Sci. Suppl. *139*, 27–33.

Serio, A., Bilican, B., Barmada, S.J., Ando, D.M., Zhao, C., Siller, R., Burr, K., Haghi, G., Story, D., Nishimura, A.L., et al. (2013). Astrocyte pathology and the absence of non-cell autonomy in an induced pluripotent stem cell model of TDP-43 proteinopathy. Proc. Natl. Acad. Sci. USA *110*, 4697–4702.

Shaltouki, A., Peng, J., Liu, Q., Rao, M.S., and Zeng, X. (2013). Efficient generation of astrocytes from human pluripotent stem cells in defined conditions. Stem Cells *31*, 941–952.

Sofroniew, M.V. (2009). Molecular dissection of reactive astrogliosis and glial scar formation. Trends Neurosci. *32*, 638–647.

Sokolova, E., Aleshin, S., and Reiser, G. (2012). Expression of protease-activated receptor (PAR)-2, but not other PARs, is regulated by inflammatory cytokines in rat astrocytes. Neurochem. Int. *60*, 276–285.

Takano, T., Tian, G.F., Peng, W., Lou, N., Libionka, W., Han, X., and Nedergaard, M. (2006). Astrocyte-mediated control of cerebral blood flow. Nat. Neurosci. *9*, 260–267.

Theodoric, N., Bechberger, J.F., Naus, C.C., and Sin, W.C. (2012). Role of gap junction protein connexin43 in astrogliosis induced by brain injury. PLoS ONE *7*, e47311.

Tom, V.J., Doller, C.M., Malouf, A.T., and Silver, J. (2004). Astrocyte-associated fibronectin is critical for axonal regeneration in adult white matter. J. Neurosci. *24*, 9282–9290.

Van Wagoner, N.J., Oh, J.W., Repovic, P., and Benveniste, E.N. (1999). Interleukin-6 (IL-6) production by astrocytes: autocrine regulation by IL-6 and the soluble IL-6 receptor. J. Neurosci. *19*, 5236–5244.

Verwer, R.W., Sluiter, A.A., Balesar, R.A., Baayen, J.C., Noske, D.P., Dirven, C.M., Wouda, J., van Dam, A.M., Lucassen, P.J., and Swaab, D.F. (2007). Mature astrocytes in the adult human neocortex express the early neuronal marker doublecortin. Brain *130*, 3321–3335.

Voutsinos-Porche, B., Bonvento, G., Tanaka, K., Steiner, P., Welker, E., Chatton, J.Y., Magistretti, P.J., and Pellerin, L. (2003a). Glial glutamate transporters mediate a functional metabolic crosstalk between neurons and astrocytes in the mouse developing cortex. Neuron *37*, 275–286.

Voutsinos-Porche, B., Knott, G., Tanaka, K., Quairiaux, C., Welker, E., and Bonvento, G. (2003b). Glial glutamate transporters and maturation of the mouse somatosensory cortex. Cereb. Cortex *13*, 1110–1121.

Wichterle, H., Lieberam, I., Porter, J.A., and Jessell, T.M. (2002). Directed differentiation of embryonic stem cells into motor neurons. Cell *110*, 385–397.

Yamanaka, K., Chun, S.J., Boillee, S., Fujimori-Tonou, N., Yamashita, H., Gutmann, D.H., Takahashi, R., Misawa, H., and Cleveland, D.W. (2008). Astrocytes as determinants of disease progression in inherited amyotrophic lateral sclerosis. Nat. Neurosci. *11*, 251–253.

Yang, Y., Vidensky, S., Jin, L., Jie, C., Lorenzini, I., Frankl, M., and Rothstein, J.D. (2011). Molecular comparison of GLT1+ and ALDH1L1+ astrocytes in vivo in astroglial reporter mice. Glia *59*, 200–207.

Yu, P.B., Deng, D.Y., Lai, C.S., Hong, C.C., Cuny, G.D., Bouxsein, M.L., Hong, D.W., McManus, P.M., Katagiri, T., Sachidanandan, C., et al. (2008). BMP type I receptor inhibition reduces heterotopic [corrected] ossification. Nat. Med. *14*, 1363–1369.

Zamanian, J.L., Xu, L., Foo, L.C., Nouri, N., Zhou, L., Giffard, R.G., and Barres, B.A. (2012). Genomic analysis of reactive astrogliosis. J. Neurosci. *32*, 6391–6410.